

# Bortezomib overcomes MGMT-related resistance of glioblastoma cell lines to temozolomide in a schedule-dependent manner

Panagiotis J. Vlachostergios · Eleana Hatzidaki ·  
Christina D. Befani · Panagiotis Liakos ·  
Christos N. Papandreou

Received: 6 February 2013 / Accepted: 24 April 2013 / Published online: 5 May 2013  
© Springer Science+Business Media New York 2013

**Summary** Development of drug resistance after standard chemotherapy for glioblastoma multiforme (GBM) with temozolomide (TMZ) is associated with poor prognosis of GBM patients and is at least partially mediated by a direct DNA repair pathway involving O6-methylguanine methyltransferase (MGMT). This enzyme is under post-translational control by a multisubunit proteolytic cellular machinery, the 26S proteasome. Inhibition of the proteasome by bortezomib (BZ), a boronic acid dipeptide already in clinical use for the treatment of myeloma, has been demonstrated to induce growth arrest and apoptosis in GBM cells. In this study we investigated the effect of sequential treatment with BZ and TMZ on cell proliferation-viability and apoptosis of the human T98G and U87 GBM cell lines. We also tested for an effect of treatment on MGMT expression and important upstream regulators of the latter, including nuclear factor kappa B (NFκB), p44/42 mitogen-activated protein kinase (MAPK), p53, signal transducer and activator of transcription 3 (STAT3) and hypoxia-inducible factor 1α (HIF-1α). The sequence of drug administration for maximal cytotoxicity favored BZ prior to TMZ in T98G cells while the opposite was the case for U87 cells. Maximal efficacy was associated with downregulation of

MGMT, reduced IκBα-mediated proteasome-dependent nuclear accumulation of NFκB, attenuation of p44/42 MAPK, AKT and STAT3 activation, and stabilization of p53 and inactive HIF-1α. Collectively, these results suggest that proteasome inhibition by BZ overcomes MGMT-mediated GBM chemoresistance, with scheduling of administration being critical for obtaining the maximal tumoricidal effect of combination with TMZ.

**Keywords** Bortezomib · Temozolomide · Glioblastoma · MGMT · NFκB · MAPK · p53 · STAT3 · HIF-1α · AKT

## Introduction

Drug resistance of glioblastoma multiforme (GBM) is a key factor involved in poor responses and dismal prognosis of this tumor, despite marginal benefits achieved after introduction of concurrent chemoradiation and adjuvant temozolomide (TMZ) as the standard of care [1]. A major player in the emergence of resistance, either as intrinsic feature of a significant proportion of GBMs or as a secondary response to alkylating agents is O6-methylguanine methyltransferase (MGMT) [2]. This direct DNA repair protein is responsible for removal of alkyl groups from damaged DNA through a one-way suicide reaction which results in MGMT proteolytic degradation by the 26S proteasome [3]. Importantly, MGMT promoter methylation has been associated with a better clinical response to chemoradiation and overall survival [4].

Regulation of MGMT is a complex process. To date, several transcription factors and coactivators have been suggested to be involved in transcriptional regulation of MGMT, including nuclear factor kappa B (NFκB), p53, hypoxia-inducible factor 1α (HIF-1α), AP-1, Sp1, glucocorticoids, cAMP response element-binding protein (CBP), p300

**Electronic supplementary material** The online version of this article (doi:10.1007/s10637-013-9968-1) contains supplementary material, which is available to authorized users.

P. J. Vlachostergios (✉) · E. Hatzidaki · C. N. Papandreou  
Department of Medical Oncology, Faculty of Medicine, School  
of Health Sciences, University of Thessaly, Biopolis,  
41110 Larissa, Greece  
e-mail: pvlacho@med.uth.gr

C. D. Befani · P. Liakos  
Laboratory of Biochemistry, Faculty of Medicine, School of  
Health Sciences, University of Thessaly, Biopolis,  
41110 Larissa, Greece

and MGMT enhancer binding protein (MEBP) [5–13]. In addition, post-transcriptional regulation of MGMT has also been reported to occur through signal transducer and activator of transcription 3 (STAT3) signaling as well as through mRNA processing by microRNAs (miR), in particular miR-181d [14, 15].

In addition to MGMT, the 26S proteasome as disposal cellular machinery is involved in degradation of several damaged or misfolded proteins within the cell [16]. Bortezomib (BZ) is a pharmacologic inhibitor of the proteasome, currently approved for clinical use in treatment of myeloma, but is also active in GBM cells, inducing growth inhibition and apoptosis through upregulation of cell cycle arrest- and proapoptotic-proteins (cyclin B1, p21, p27, Bmf, TRAIL DR5), enhancement of TRAIL-mediated apoptosis, downregulation of cell cycle progression- and antiapoptotic- proteins (CDK2, CDK4, E2F4, Bcl-2, Bcl-xl), and activation of JNK signaling [17–20].

The concept of proteasome inhibition as a strategy to overcome glioma chemoresistance is currently being tested at the clinical level, with reported results from two phase I studies of BZ and TMZ, as well as ongoing phase II studies [21, 22]. However, the molecular mechanisms underlying this drug combination have not been elucidated. In this work, we investigated the effect of sequence-dependent combinations of TMZ and BZ on proliferation-viability and apoptosis of high (T98G) and low (U87) MGMT-expressing GBM cells, looking for an effect on MGMT and important upstream MGMT regulators, including NF $\kappa$ B, p44/42 mitogen-activated protein kinase (MAPK), p53, STAT3 and HIF-1 $\alpha$ . Our results indicate that BZ exerts a chemosensitizing effect which is unique for each GBM cell line, depending on the order of administration. The mechanism of this dependency involves downregulation of MGMT through interference with NF $\kappa$ B, MAPK, STAT3 and HIF-1 $\alpha$  signaling pathways and offers a rationale for their assessment as predictors of response in future trials and as therapeutic targets.

## Materials and methods

### Cell culture and reagents

The human GBM cell lines T98G (p53 mutant, p53mt) and U87 (p53 wild-type, p53wt) were purchased from the European Collection of Animal Cell Cultures (ECACC, UK) and all experiments were performed within 6 months from purchase. The cell lines were cultured in Dulbecco's modified Eagle's medium (GIBCO, UK) supplemented with 10 % heat-inactivated FBS (GIBCO, UK), 5 % L-glutamine (GIBCO, UK) and 1 % penicillin-streptomycin (Euroclone, UK) at 37 °C in a humidified 5 % CO<sub>2</sub> atmosphere. TMZ (Merck, UK) was dissolved in dimethyl sulfoxide (DMSO)

at a concentration of 100 mM, stored as a stock solution at –80 °C and diluted in culture medium just before use. BZ (Janssen-Cilag, Greece) was dissolved in deionized water and diluted in culture medium just before use. For BZ pretreatment experiments, cells were treated with 0.1  $\mu$ M BZ for 24 h. The BZ-containing medium was then removed and cells were washed twice with PBS. Then, cells were treated with either fresh medium or medium containing 100  $\mu$ M TMZ for 16 h. For delayed BZ treatment, cells were incubated in TMZ-containing medium for 16 h. Then, cells were treated with either fresh medium or medium containing 0.1  $\mu$ M BZ for 24 h (Fig. 1a). The final concentration of DMSO in culture medium was <0.1%v/v. A 0.1 % DMSO vehicle for 16 h was used as a negative control for TMZ.

### 3-(4,5-dimethylthiazol-2-yl)-2,5-diphenyltetrazolium bromide (MTT) assay

Cells were plated in 96-well plates at a density of  $2 \times 10^5$ . Cells were allowed to attach for 24 h at 37 °C and were then treated with the drug combinations, as described previously. After treatment, 10 mL of MTT reagent (R&D Systems, UK) were added in each well, and plates were further incubated for 4 h at 37 °C. Then, 100 mL of MTT detection reagent (R&D Systems, UK) were added in each well, and plates were left at room temperature overnight, protected from light. Samples were analyzed at a wavelength of 570 nm with a reference at 650 nm in a 1420 Victor device (Wallac Victor, Finland). Experimental wells were carried out in triplicate ( $p < 0.01$ ).

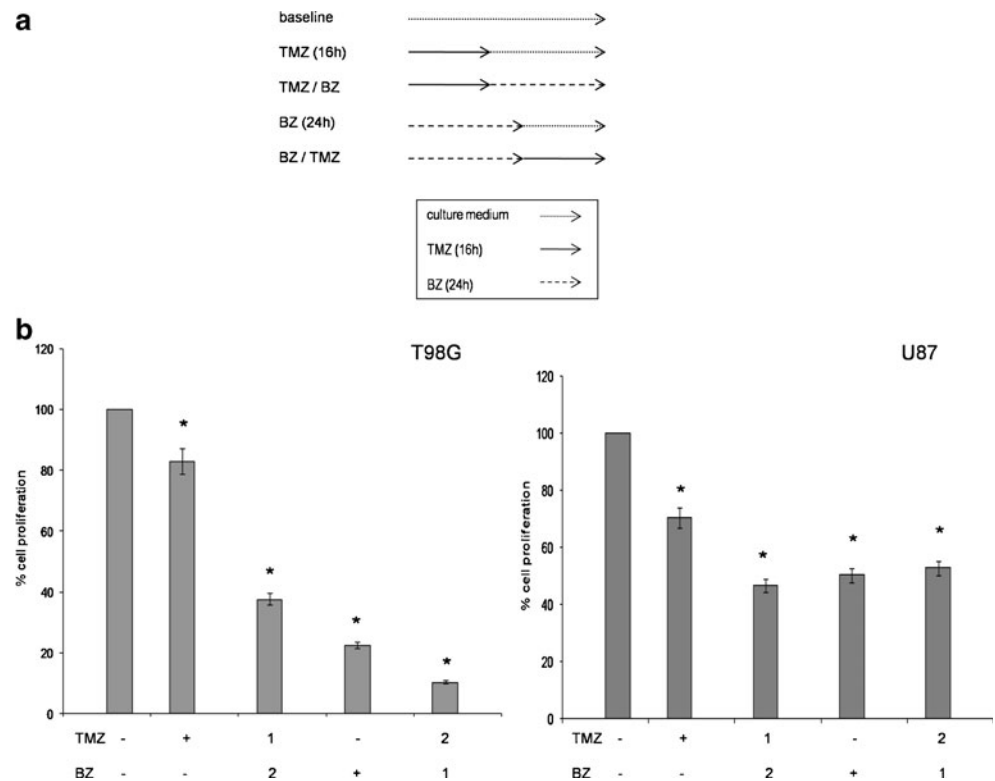
### Drug combination interaction analysis

The interaction of the two-drug combinations, in the two cell lines, was analysed with the use of ratio R from the MTT assay data, as previously reported [23, 24]. The ratio R is calculated as follows:  $R = \text{Survival}[\text{Combination}] / \text{Survival}[\text{TMZ}] \times \text{Survival}[\text{BZ}]$ . If R is less than 0.8 the combination is considered synergistic, if it is between 0.8 and 1.2, the combination is considered additive, and if R is more than 1.2 the combination is considered antagonistic.

### DNA fragmentation

DNA fragmentation was determined using the cellular DNA fragmentation ELISA kit (Roche Diagnostics, Germany). After exposure to bromodeoxyuridine (BrdU) for 18 h, cells were reseeded onto a microplate ( $10^5$  cells/well) and treated with the drug combinations, as described previously. Supernatant was removed and remaining cells were lysed with the kit buffer. Cell lysate was transferred into an anti-DNA pre-coated microtiter plate and analyzed using the ELISA

**Fig. 1** Effect of BZ and TMZ on proliferation-viability of T98G and U87 cells. **a** Schema of treatment regimens. **b** MTT assay. Numbers 1, 2 illustrate the order of addition of each drug. For BZ pretreatment experiments, cells were treated with 0.1  $\mu\text{M}$  BZ for 24 h. The BZ-containing medium was then removed and cells were washed twice with PBS. Then, cells were treated with either fresh medium or medium containing 100  $\mu\text{M}$  TMZ for 16 h. For delayed BZ treatment, cells were incubated in TMZ-containing medium for 16 h. Then, cells were treated with either fresh medium or medium containing 0.1  $\mu\text{M}$  BZ for 24 h. Results represent the mean ( $\pm$ SEM) of three independent experiments performed in triplicate ( $*p < 0.01$ ; baseline vs treated cells)



procedure. After 1 h of incubation, exonuclease treatment was carried out during 30 min. DNA fragmentation was measured spectrophotometrically (at 450 nm and 690 nm as the reference wavelength) after the anti-BrdU-peroxidase conjugate and the substrate solutions had been added. BrdU-labeled fragments measured in cell lysate denoted apoptotic fragmentation. A positive control was prepared for each cell line to obtain a relative quantification of the amount of apoptosis in each treatment condition. According to the manufacturer's instructions (Roche Diagnostics, Germany), this was performed after solubilization of genomic DNA by endogenous nucleases. The results presented are the mean values of three independent experiments ( $p < 0.01$ ).

#### Western blot analysis

Fractionation of cells, analysis of nuclear and cytoplasmic fractions, or total cellular proteins, and electrophoresis were carried out as previously described [25]. Primary antibodies against the p65 subunit of NF $\kappa$ B, I $\kappa$ B $\alpha$ , p53, caspase-3, STAT3 (Santa Cruz Biotechnology, USA), human HIF-1 $\alpha$  (BD Biosciences, USA), phospho-p44/42 MAPK (Erk1/2) (Thr 202/Tyr 204), p44/42 MAPK (Erk1/2), phospho-AKT (Ser 473), total AKT, phospho-STAT3 (Tyr705) (Cell Signaling, USA), Histone 2B (Abcam, UK), and actin (Sigma Aldrich, UK) were used. Horseradish peroxidase-conjugated secondary antibodies were obtained from Santa Cruz Biotechnology, USA. Densitometric analysis of the

bands in blots was carried out with the public domain software for image analysis "ImageJ" (National Institute of Health, USA). All experiments were carried out in triplicate ( $p < 0.01$ ) and representative results are shown. Bar graphs of relative expression results from three independent experiments are provided in [Supplementary files](#).

#### Immunofluorescence

Cells were grown on coverslips, washed once with PBS, and fixed with 3 % formaldehyde in PBS for 5 min at room temperature. Cells were washed twice with PBS and permeabilized with PBS containing 0.1 % Triton X-100 for 15 min. After being washed twice with PBS cells were treated with 3 % BSA in PBS for 1 h. Coverslips were incubated for 1 h at room temperature with a monoclonal anti-p65 antibody (Santa Cruz Biotechnology, USA), washed twice with PBS, and incubated for 1 h at room temperature with FITC-conjugated (Bio-Rad, USA) secondary antibodies. After being washed twice with PBS, cells were counterstained with 4',6-diamidino-2-phenylindole (DAPI) mounted on slides, viewed on an Axioscope 40 Zeiss microscope and recorded by a Leica DFC480 camera.

#### 20S proteasome activity assay

Total protein cell lysates were prepared using a 0.5 % CHAPS buffer which did not affect proteasomal enzymatic activity. Chymotryptic activity of the 20S proteasome was

measured in total cell lysates as previously described [25]. All measurements were performed in triplicate ( $p < 0.01$ ).

#### Reverse transcription polymerase chain reaction (RT–PCR)

Total RNA was isolated from T98G cells using a commercial RNA isolation kit (Bio-Rad, USA). Using 1  $\mu$ g total RNA, single-stranded DNA (cDNA) was synthesized by the use of a cDNA synthesis kit (Bio-Rad, USA). The primers used were, for MGMT forward, AGAGTCGTTCCACCAGACAGG and MGMT reverse, GCCATTCCTTCACGGCCAG. Glyceraldehyde-3-phosphate dehydrogenase (GAPDH) gene expression was used as a loading control, with primers for GAPDH forward, GGA AGG TGA AGG TCG GAG TCA and GAPDH reverse, GTC ATT GAT GGC AAC AAT ATC CAC, respectively. Conditions for MGMT were 35 cycles, Tanneal 55 °C and for GAPDH were 35 cycles, Tanneal 58 °C. PCR products were subjected to electrophoretic analysis on 2 % agarose gels containing ethidium bromide (Sigma Aldrich, UK), and were visualized and photographed under UV light. Treatment conditions were as described above. All experiments were carried out in triplicate ( $p < 0.01$ ) and representative results are shown.

#### Statistical analysis

The Graph Pad InStat Statistical package for Windows (GraphPad Software, USA) was used. Data are expressed as mean  $\pm$  SEM. The one-way analysis of variance (ANOVA) with the Bonferroni post-test was used for the comparison of data, and the statistical significance limit was set at  $p < 0.05$ .

## Results

BZ increases the inhibitory effect of TMZ on proliferation-viability of GBM cells in a schedule-dependent manner

The ultimate mechanism of TMZ action involves initiation of apoptotic signaling after unrepaired alkylation DNA damage. However, glioma cells may evade cell death in response to TMZ by undergoing prolonged G2/M arrest [26, 27]. BZ exposure was also found to increase the percentage of cells in the G2/M phase [17]. Based on these data, we postulated that consecutive rather than concurrent combination of the drugs might be more appropriate for eliciting tumoricidal effects. Also, given the central role of NF $\kappa$ B in the MGMT-related response of gliomas to O6-alkylating agents as well as in mediating the anticancer effects of BZ [10, 28, 29], we hypothesized that doses of TMZ and BZ with an established inhibitory effect on NF $\kappa$ B might result in greater treatment efficacy when used in combination (Fig. 1a). Thus, the concentration and time of TMZ administration (100  $\mu$ M

for 16 h) was selected based on previous evidence of increased cytotoxicity associated with maximal inhibition of NF $\kappa$ B transcriptional activity, in the same cell lines [30]. Likewise, the concentration and time of BZ administration (0.1  $\mu$ M for 24 h) was selected based on data supporting initiation of apoptosis associated with reduction of nuclear NF $\kappa$ B levels and transcriptional activity, in the same cell lines [17].

To assess the proliferation-viability of cells exposed to either drug alone or the combinations we performed an MTT assay. We observed that both drugs exerted a growth inhibitory effect on either cell line, with BZ monotherapy being more effective compared to TMZ alone. T98G were seemingly more susceptible to BZ antiproliferative action compared to U87 cells. The order of drug administration in the combination schedules elicited different responses in the two cell lines. In T98G cells, BZ prior to TMZ was more active than BZ alone, which in turn was more effective compared to TMZ followed by BZ. In contrast, U87 cells displayed greater sensitivity to early administration of TMZ followed by BZ, and this schedule induced growth arrest and inhibition of cell proliferation-viability to a greater extent compared to BZ monotherapy, and BZ prior to TMZ, in descending order. TMZ monotherapy was the least effective among all treatment conditions in both cell lines (Fig. 1b). 0.1 % DMSO vehicle had no effect on cell proliferation-viability in either cell line (data not shown).

We performed a drug combination interaction analysis based on MTT data and found that in both cell lines, all drug combinations between TMZ and BZ displayed a synergistic effect. However, in T98G cells synergy was more pronounced in the early BZ treatment before TMZ compared to the delayed BZ administration after TMZ, whereas in U87 cells the opposite was the case for the corresponding drug combination schedules (Table 1).

BZ induces apoptosis in TMZ-treated GBM cells in a schedule-dependent manner

To explore whether BZ-mediated reduction of cell proliferation-viability is associated with apoptotic death, we tested for presence of cleaved caspase-3 fragments under the same conditions. We observed that TMZ monotherapy

**Table 1** R value for the combination of TMZ (100  $\mu$ M 16 h) and BZ (0.1  $\mu$ M 24 h) in T98G and U87 cells

Cell line	R value $\pm$ SEM	
	BZ(1)/TMZ(2)	TMZ(1)/BZ(2)
T98G	0.006 $\pm$ 0.001	0.023 $\pm$ 0.005
U87	0.015 $\pm$ 0.001	0.013 $\pm$ 0.001

had no significant effect on caspase-3 in either cell line. In contrast, BZ alone resulted in increased caspase-3 cleavage in both cell lines. When combined with TMZ, the order of BZ addition led to different outcomes in cell fate of the two cell lines. T98G cells displayed pronounced caspase-3 cleavage after the early BZ schedule, whereas they showed no significant increase in caspase-3 fragments with the late BZ schedule. In contrast, the exact opposite effects in terms of drug sequencing were observed in U87 cells (Fig. 2a).

To confirm and quantify our results on apoptosis, we performed a DNA fragmentation ELISA assay under the same conditions. We observed a dependency of the magnitude of apoptotic fragmentation (compared to positive controls of each cell line) on the order of BZ addition to TMZ. In T98G cells, BZ monotherapy induced apoptotic rates as high as BZ followed by TMZ, and both schedules were comparable with the positive control (CTL). Delayed BZ after TMZ induced less apoptosis than the previous

conditions but greater than TMZ alone. In U87 cells, TMZ followed by BZ was the strongest apoptosis-inducing schedule, followed by BZ. Early BZ prior to TMZ was not as effective as late BZ treatment but induced more apoptotic fragmentation compared to TMZ alone (Fig. 2b). 0.1 % DMSO vehicle had no effect on apoptosis in either cell line (data not shown).

BZ reduces TMZ-induced MGMT and proteasome-dependent I $\kappa$ B $\alpha$ -mediated nuclear accumulation of NF $\kappa$ B in a schedule-dependent manner

To test our hypothesis that BZ-induced sensitization to TMZ might result from inhibition of NF $\kappa$ B-dependent, MGMT-mediated DNA repair we assessed the levels and intracellular localization of these two proteins, under the same conditions. We observed that TMZ increased nuclear accumulation of both NF $\kappa$ B and MGMT in both cell lines.

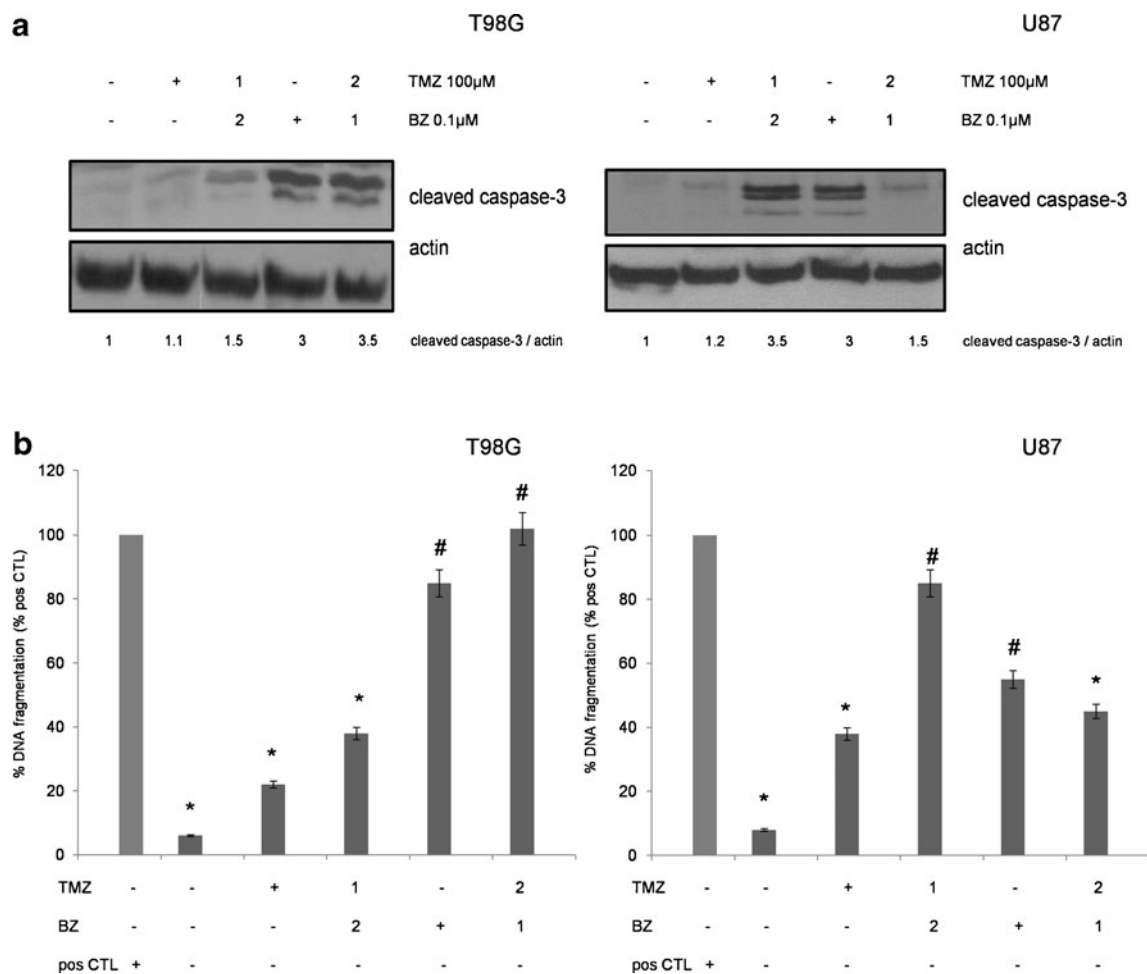


**Fig. 2** Effect of BZ and TMZ on apoptosis of T98G and U87 cells. **a** Western blotting of total lysates from T98G (left) and U87 cells (right) for caspase-3 fragments incubated as in Fig. 1b. **b** DNA fragmentation ELISA of lysates from T98G (left) and U87 cells (right) measured as % percentage of BrdU DNA fragments of treated cells compared to

positive control (CTL), incubated as in a. Results represent the mean  $\pm$ SEM of three independent experiments performed in triplicate (\* $p$  < 0.01; baseline vs treated cells, # $p$  < 0.01; TMZ vs BZ and TMZ vs combination)

In contrast, BZ had the opposite effects, causing a significant reduction of nuclear NF $\kappa$ B and MGMT levels as well as an increase in cytoplasmic NF $\kappa$ B levels. MGMT, being a nuclear DNA repair enzyme, was undetectable in the cytoplasm in all experimental conditions [31]. Again, when combined, TMZ and BZ were able to reduce nuclear NF $\kappa$ B and MGMT only in an order-dependent fashion that was reverse between T98G and U87 cells, favoring early BZ incubation for T98G and delayed BZ addition for U87 cells (Fig. 3a).

To further test our hypothesis on the modulation of the NF $\kappa$ B-MGMT response after treatment, we performed a qualitative assessment of MGMT transcript levels with RT-PCR in the high MGMT expressing T98G cell line, under the same conditions. We also assessed intracellular NF $\kappa$ B localization with indirect immunofluorescence microscopy, in both cell lines. We found that TMZ significantly induced MGMT mRNA but this effect was prevented with addition of BZ, seemingly more efficiently in the early compared to late administration of BZ in relation to TMZ (Fig. 3b). With regard to NF $\kappa$ B, a mixed pattern of nuclear and cytoplasmic NF $\kappa$ B was observed at baseline, whereas TMZ led to an increase of nuclear NF $\kappa$ B amount, in both cell lines. In contrast, BZ reduced NF $\kappa$ B nuclear accumulation. With regard to the combination of the drugs, an inverse result was produced in the two cell lines depending on the order of administration. In T98G cells, delayed BZ addition after TMZ resulted in increased NF $\kappa$ B nuclear accumulation whereas early BZ incubation before TMZ led to a cytoplasmic localization pattern. In U87 cells, delayed BZ schedule decreased nuclear NF $\kappa$ B amount whereas early BZ before TMZ favored NF $\kappa$ B nuclear accumulation (Fig. 3c).

Then we tested whether the aforementioned effects of treatment on NF $\kappa$ B are mediated through proteasomal activity-dependent modulation of I $\kappa$ B levels. We observed that TMZ led to an increase in 20S proteasome activity which was more pronounced in U87 cells compared to T98G cells and was accompanied by reduction of I $\kappa$ B $\alpha$  levels. BZ either alone or in combination with TMZ reduced proteasome activity thereby stabilizing I $\kappa$ B $\alpha$  levels in both cell lines. Maximal inhibition of proteasome activity was unique for each cell line and was accompanied by maximal propagation of I $\kappa$ B $\alpha$  accumulation, at the same treatment schedules that resulted in greatest attenuation of nuclear NF $\kappa$ B localization, as described above (Fig. 3d).

**BZ inhibits TMZ-induced MAPK and STAT3 signaling and stabilizes wt p53 in a schedule-dependent manner**

To test the effects of treatment on signaling pathways other than NF $\kappa$ B, which also regulate MGMT expression, we assessed the phosphorylated and total levels of MAPK and STAT3 proteins and total levels of p53. We found that TMZ

enhanced phosphorylation-dependent activation of MAPK and STAT3, whereas BZ reduced their phosphorylated counterparts compared to the total protein levels which were not affected in either cell line. In T98G cells, BZ prior to TMZ led to greater inhibition of MAPK and STAT3 phosphorylation compared to late BZ incubation after TMZ. In U87 cells, the TMZ/BZ schedule inhibited MAPK and STAT3 phosphorylation more potently compared to the BZ/TMZ schedule (Fig. 4a). Levels of mt p53 were not appreciably changed by either drug of their combinations in T98G cells compared to baseline (data not shown). However, p53 accumulation was observed in U87 cells in response to BZ treatment, which was slightly greater when TMZ was added prior to BZ. In contrast, p53 levels after early BZ administration followed by TMZ were not appreciably changed (Fig. 4a).

**BZ promotes HIF-1 $\alpha$  accumulation but inhibits AKT-dependent HIF-1 $\alpha$  translation and nuclear MAPK-dependent HIF-1 $\alpha$  activation**

When we assessed HIF-1 $\alpha$ , which is an inducer of MGMT transcription, we observed that BZ stabilized HIF-1 $\alpha$  protein levels at the same treatment conditions which were previously found to downregulate MGMT. These included BZ and BZ/TMZ exposures for T98G, and TMZ/BZ, BZ for U87 cells. The effect was more pronounced in U87 cells but was also observed in T98G cells to a lesser extent (Fig. 4b). This prompted us to further investigate for evidence of actual HIF-1 $\alpha$  activation. Thus, we checked the phosphorylated and total levels of AKT, which is known to promote HIF-1 $\alpha$  translation in GBM [32]. In addition we tested the phosphorylated and total nuclear amount of MAPK, which is responsible for HIF-1 $\alpha$  nuclear translocation and transcriptional activity, as shown in other cancer cell types [33, 34]. We found that in a schedule-dependent, cell-specific way, effective treatment conditions in terms of MGMT inhibition also led to decreased phosphorylation of both AKT and nuclear MAPK, thus implying that the accumulated HIF-1 $\alpha$  was functionally inactive (Fig. 4b).

## Discussion

Despite the growing number of molecular mechanisms implicated in TMZ resistance of GBM, methylation of MGMT gene promoter remains the only established molecular marker linked to sensitivity to alkylating agent chemotherapy [35]. However, accumulating clinical evidence implicates several signaling pathways in determination of responses and outcomes of such patients. Tumor necrosis factor- $\alpha$ -induced protein 3 (TNFAIP3) was identified as regulatory component of a putative cytoplasmic signaling cascade that mediates NF $\kappa$ B activation in response to DNA damage caused by O6-alkylating

**Fig. 3** Effect of BZ and TMZ on nuclear NFκB, MGMT expression, total IκBα and 20S proteasome activity of T98G and U87 cells. **a** Western blotting of nuclear and cytoplasmic lysates from T98G (left) and U87 cells (right) for NFκB and MGMT, incubated as in Fig. 1b. Histone 2B served as nuclear marker while actin served as cytoplasmic marker. **b** RT-PCR of MGMT mRNA in T98G cells incubated as in a. GAPDH was used as a loading control. **c** Immunofluorescence microscopy of T98G (upper) and U87 cells (lower) for NFκB and U87 cells (lower) for NFκB incubated as in a. Nuclei were stained with 4',6-diamidino-2-phenylindole (DAPI). Magnification bars=10 μM. **d** 20S proteasome activity assay of lysates from T98G (left) and U87 cells (right) incubated as in a. 20S proteasome activity was calculated as RFU/μg and expressed as % percentage of baseline. Results represent the mean ±SEM of three independent experiments performed in triplicate (\**p*<0.01; baseline vs treated cells). Western blotting of total lysates from T98G (left) and U87 cells (right) for IκBα, incubated as in a. Actin served as loading control

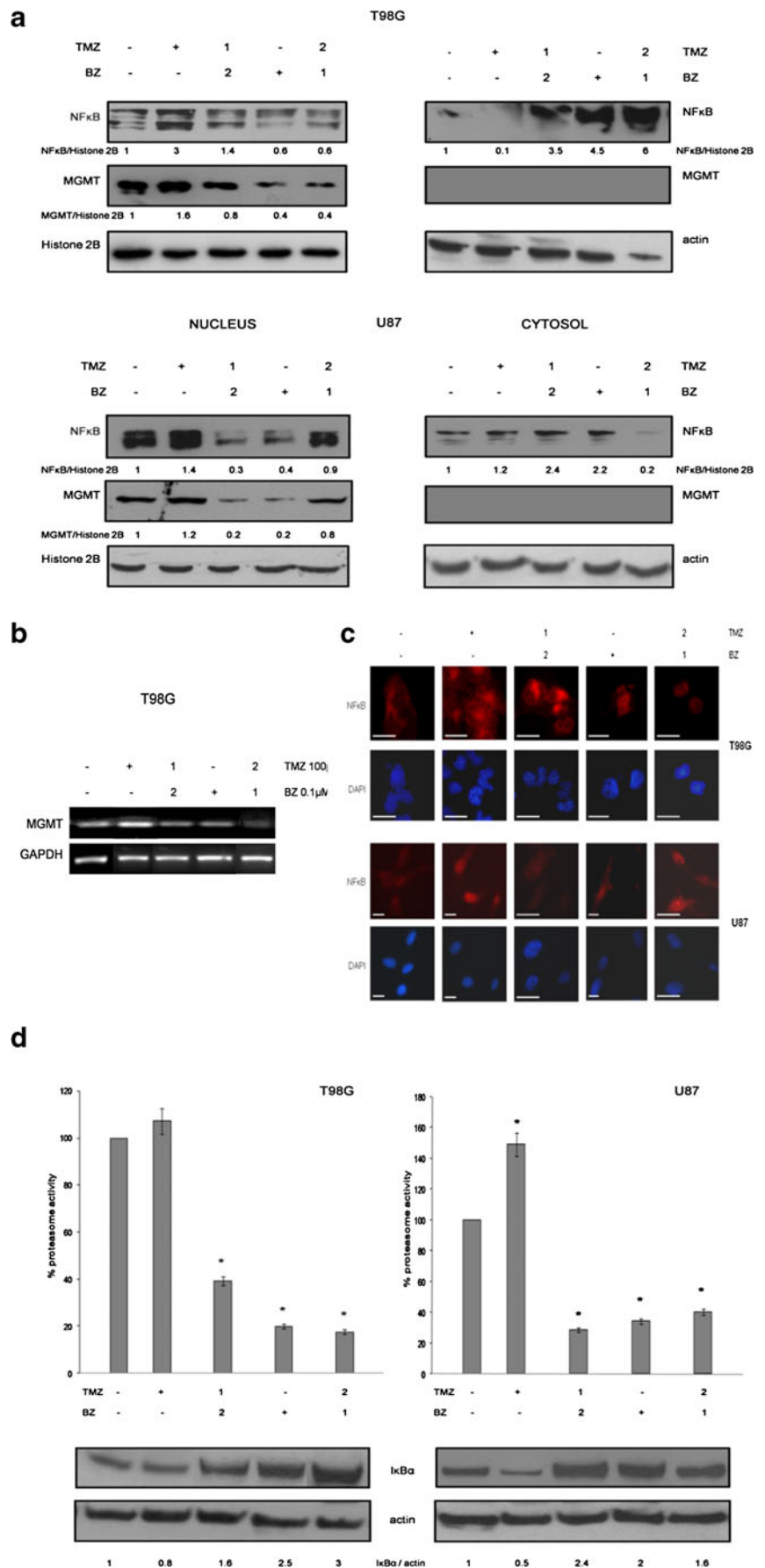
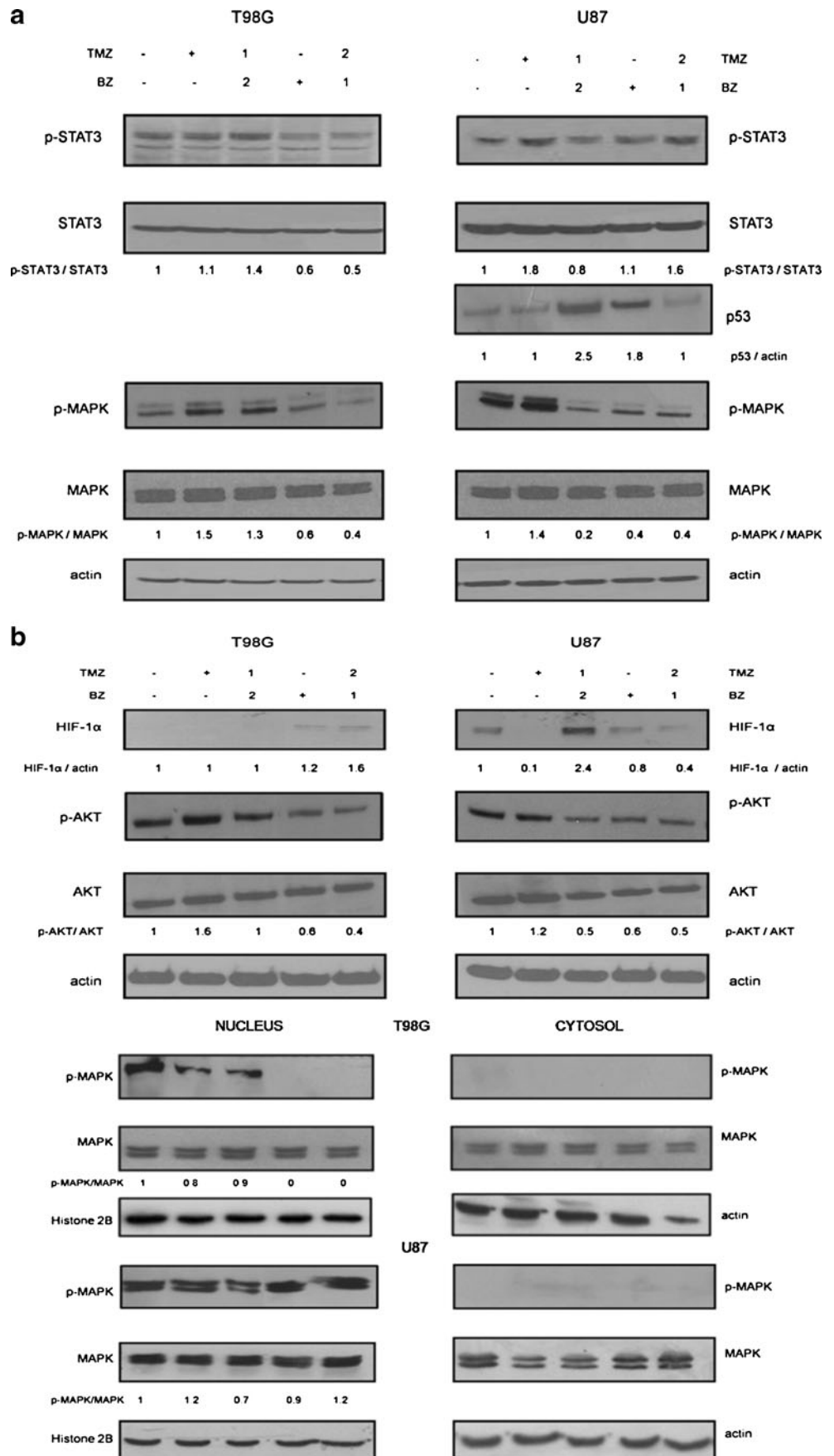


**Fig. 4** Effect of BZ and TMZ on activity of STAT3, MAPK/p53 and HIF-1 $\alpha$  pathways in T98G and U87 cells. **a** Western blotting of total lysates from T98G (*left*) and U87 cells (*right*) for p-STAT3, total STAT3, wt p53, p-MAPK and total MAPK, incubated as in Fig. 1b. Actin served as loading control. **b** Western blotting of total lysates from T98G (*left*) and U87 cells (*right*) for HIF-1 $\alpha$ , p-AKT, total AKT and of nuclear and cytoplasmic lysates for p-MAPK and total MAPK, incubated as in a. Histone 2B served as nuclear marker while actin served as cytoplasmic marker





agents [28]. Further, assessment of nuclear NF $\kappa$ B 1/p53 expression was found to be a negative prognosticator in astrocytomas of all grades [36]. Also, increased expression of phosphorylated MAPK and AKT is a predictor of poor prognosis, while activated STAT3 expression also predicts survival in such patients [37–39]. Finally, HIF-1 $\alpha$  has emerged as a useful prognostic factor in astrocytic tumors associated with necrosis on MR images and has been proposed to refine the prognostic information provided by grade [40, 41].

Intriguingly, all the above-mentioned markers not only are greatly involved in MGMT regulation either at gene or/and at protein level, but they also represent drugable targets [5, 10, 12–14]. We postulated that proteasome inhibition might be a reasonable strategy to test for sensitizing GBM cells to TMZ as it has been previously shown to inhibit these pathways either in GBM [17] or in other cancer cell types [34, 42]. Our presenting data support that the combination of TMZ and BZ is indeed active in terms of attenuating proliferation-viability and inducing apoptosis in GBM cells with variable level of MGMT expression, however the order of drug administration elicits different molecular responses which modulate tumoricidal effects. The interaction between TMZ and BZ is synergistic. However, T98G cells seem to be more sensitive to BZ compared to U87 cells when used as single agent. Reversely, U87 cells are seemingly more sensitive to TMZ compared to T98G cells. With regard to treatment combinations, interaction between early BZ and TMZ is most synergistic in T98G cells, whereas delayed BZ and TMZ is most synergistic in U87 cells. We thus tested whether treatment-induced changes in the above mentioned MGMT-regulating pathways might explain this differential, schedule-dependent drug sensitivity and synergism between the two cell lines.

First, in line with previous reports, we show that TMZ causes activation of the canonical NF $\kappa$ B pathway through increased proteasome activity-dependent I $\kappa$ B $\alpha$  reduction, and enhances activation of MAPK, STAT3 and AKT signaling in both cell lines [10, 12, 34, 38]. These effects were in parallel with an increase in MGMT nuclear levels in both cell lines and in MGMT transcript level tested in T98G cells. Under DNA damage-induced stress conditions, dependence of the MGMT protein amount to gene transcription may become stronger given that this suicide enzyme is targeted for proteolytic degradation after a 1:1 reaction with methylated DNA [3]. Thus, it is no surprise that MGMT protein levels do not decline with increasing proteasome activity. This increase in MGMT emanates, at least partially, from transcriptional induction and post-transcriptional stabilization, mediated by the afore-mentioned factors. In addition, TMZ led to a decrease in HIF-1 $\alpha$  protein levels in U87 cells, possibly through increasing HIF-1 $\alpha$  proteolytic degradation, given the extremely short half-life of the protein under normoxic conditions [43].

Second, we demonstrate that BZ treatment has greater antitumor effects compared to TMZ, significantly reducing

cell proliferation-viability and inducing p53-independent apoptosis in both cell lines, to a slightly greater extent in T98G compared to U87 cells, in accordance with previous data [17]. Further to the existing reports on antitumor mechanisms of BZ in GBM cells [17–20], we show that its antiproliferative and proapoptotic action in both T98G and U87 cell lines is exerted, at least partially, through downregulation of MGMT. At the transcriptional level, this is effected via reduced nuclear accumulation of NF $\kappa$ B as well as reduced activation of MAPK. With regard to the latter, given the p53 mutational status of T98G cells, it cannot be supported that the MAPK/Mdm2/p53 pathway is active in these cells, but only in U87 cells with functional wt p53. However, MAPK may still be involved in NF $\kappa$ B activation through I $\kappa$ B kinase (IKK) phosphorylation-dependent I $\kappa$ B degradation, and same is the case for AKT, phosphorylation levels of which are also significantly reduced by BZ [44]. At the post-transcriptional level, BZ reduces STAT3 activation and resultant MGMT upregulation [14]. However, the fact that phosphorylated STAT3 levels were shown to partially recover after addition of the proteasome inhibitor MG132 to a STAT3 inhibitor, in that study, implies that BZ may cause STAT3 inhibition in a way possibly unrelated to its proteasome inhibitory action. It is presently not possible to tell whether BZ blocks STAT3, MAPK and AKT pathways directly (e.g. as a kinase inhibitor) or indirectly through unknown proteasome substrates. In cell types other than glioma, it has been demonstrated that cancerous inhibitor of protein phosphatase 2A (CIP2A), a cellular inhibitor of protein phosphatase 2A (PP2A), mediates the effect of BZ on phospho-AKT and apoptosis; however, in GBM cells this remains elusive [45]. Considering BZ-mediated MGMT downregulation, it may initially seem contradicting that BZ led to a slight increase of previously undetected HIF-1 $\alpha$  protein levels in T98G cells, and stabilization of HIF-1 $\alpha$  protein levels in U87 cells. However, BZ effectively inhibited AKT activation and nuclear MAPK accumulation and activation which are indispensable for HIF-1 $\alpha$  protein *de novo* synthesis, nuclear targeting and transcriptional activity, respectively [33, 34]. Thus, BZ essentially inhibits transcription of HIF-1 $\alpha$  target genes, including MGMT.

Finally, we found that early BZ treatment effectively prevents the antiapoptotic response of T98G cells to TMZ, but does not significantly enhance cytotoxicity of TMZ in U87 cells compared to the reverse combination or BZ alone. In contrast, late BZ administration enhances the proapoptotic result induced after TMZ in U87 cells, but is not so efficient in reversing TMZ resistance in T98G cells compared to the reverse combination or BZ monotherapy. These observations suggest a pattern of BZ-induced sensitization to TMZ which is inverse between T98G and U87 cells, and depends on the order of drug addition. There is one previous report addressing the issue of sequencing of

TMZ and BZ in GBM [46]. In their work, Ng et al. suggest that BZ should be administered after TMZ in U87 cells due to an enhanced tumoricidal effect compared to either early BZ administration or concurrent treatment with both drugs. They replicated their results with other proteasome inhibitors as well as in an *in vivo* xenograft model [46]. Despite differences in dosing and time schedules, our data are in line with their results. To explain this dependency on the order of drug administration they performed an analysis of cell cycle distribution, which however showed no alterations by different order of BZ addition with regard to TMZ (although they observed increased mitotic arrest with morphological criteria). They postulated that DNA damage-induced upregulation of DNA repair might be a plausible explanation [46].

Our results complement their work by showing that the mechanism underlying this dependency involves indeed MGMT, which is a critical DNA repair pathway involved in alkylation damage, with established clinical significance. Thus, maximal downregulation of MGMT seems to indicate the most effective sequence in both cell lines. Furthermore, the implication of MGMT in determination of response to the BZ-TMZ combination extends to all major signaling pathways involved in MGMT regulation, including NF $\kappa$ B, MAPK, STAT3 and HIF-1 $\alpha$  pathways (Fig. 5). As such, changes in the nuclear and cytoplasmic localization of NF $\kappa$ B and MAPK, and phosphorylation status of MAPK, AKT and STAT3 are in accordance with MGMT levels and are also indicative of resistance or response, depending on

the order of drugs. p53 cellular status is probably not implicated in initiation of apoptosis as both p53 wt and p53 mt were able to undergo programmed cell death, as previously reported [26]. However in p53-proficient U87 cells, p53 accumulation paralleled the cytotoxic effect of BZ either alone or after TMZ pretreatment, whereas inability to raise p53 levels predicted reduced sensitivity to either TMZ alone or BZ addition prior to TMZ, thus implying that the MAPK/p53 axis may be active in this case.

Based on these results, we propose two putative models of TMZ resistance and expected response to the combination of TMZ and BZ. The first model, simulating T98G cells, features inherent baseline upregulation or/and a potential for activation of MGMT and upstream pathways involving NF $\kappa$ B, MAPK, STAT3 and HIF-1 $\alpha$ . In this case, administration of TMZ first might not seem an effective strategy. Instead, pretreatment with BZ, which is a potent inhibitor of these pathways determining alkylation resistance might enable sensitization to TMZ, thus maximizing its effects. The second model, simulating U87 cells, is characterized by low baseline levels of MGMT and its upstream pathways, which might permit treatment initiation with TMZ but would also require BZ as a second drug to reverse the expected upregulation of DNA repair resulting from induced DNA damage. Nonetheless, it cannot be excluded that the mechanism of sensitization through NF $\kappa$ B, MAPK, STAT3 and HIF-1 $\alpha$  inhibition may not be totally MGMT-dependent as these factors have been associated with resistance of GBM to treatment irrespectively of MGMT status [30, 38, 40, 47]. Also, the effectiveness of TMZ on glioma cells has largely been established in relation to MGMT promoter methylation and not necessarily to MGMT protein expression, although the latter was also shown to predict slower tumor progression in GBM patients [48–50].

In our study we did not assess the status of MGMT methylation under the experimental conditions used. First, despite the fact that methylation is involved in silencing of the MGMT gene in tumors, regulation of MGMT expression is a more complex process determined by several factors, including transcription modifiers and post-translational protein modifications which were the primary aim of this investigation. Second, variations in the methylation pattern of discrete CpG sites have been observed in pyrosequencing and methylation-specific PCR (MSP) studies, suggesting that not all CpG islands are of equal significance for silencing of MGMT, let alone that hemimethylated cell lines and tumors represent a unique entity [51]. Thus, the ideal combinations of methylated CpGs that would be better predictors of TMZ sensitivity due to MGMT gene silencing are still under investigation [52]. More importantly, up-regulation of MGMT without concomitant change in promoter methylation has been reported in recurrent tumors, indicating that mechanisms other than CpG methylation

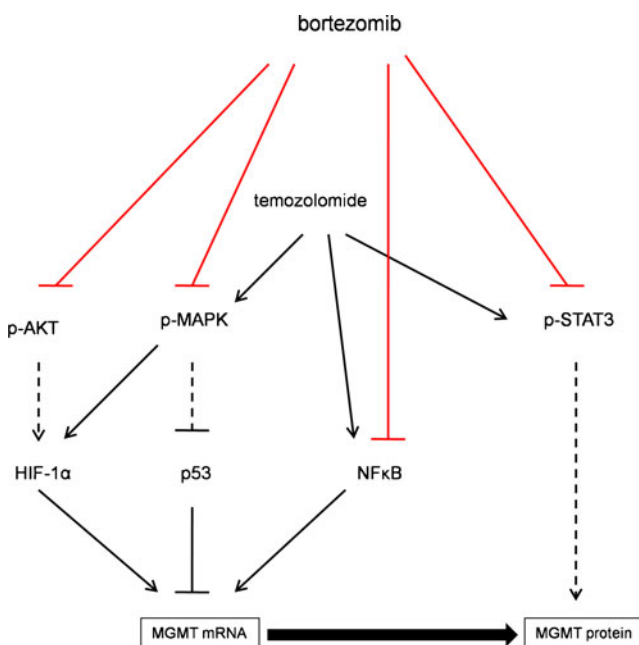


**Fig. 5** Schematic model of the possible mechanisms of BZ-mediated inhibition of TMZ-induced MGMT expression. *Continuous lines* stand for transcriptional regulation while *dash lines* stand for post-transcriptional regulation of MGMT

may also be involved in MGMT regulation during progression after treatment [51]. Intriguingly, MGMT protein expression more than the level of MGMT promoter methylation was found to predict the response to TMZ in human tumour cell lines, including T98G [52]. In another in vitro study, exposure of T98G cells in higher concentrations of TMZ for longer incubation times compared to ours, failed to demonstrate any changes in MGMT methylation status of either wild or transfected cells with liver-type glutaminase (LGA), which downregulates MGMT [53].

In the clinical setting, MGMT promoter methylation status does not change from the primary to recurrent tumors in the majority of glioblastoma patients [54], and any observed changes after recurrence are not predictive of outcome [55]. Notably, discordant findings in MGMT methylation and lack of correlation with expression of DNA-methyltransferases (DNMTs), which are the regulatory enzymes for DNA methylation patterns in eukaryotic cells, indicate methylation-independent pathways of MGMT expression regulation [56]. In contrast, low MGMT mRNA expression emerged as an independent favorable predictor of time to progression, treatment response, and survival [56].

In conclusion, we have revealed a new role for BZ as a potent MGMT inhibitor in GBM through interference with NF $\kappa$ B, MAPK, STAT3 and HIF-1 $\alpha$  pathways. In this context, we have further shown that addition of BZ to TMZ overcomes alkylation resistance in a strictly order-dependent fashion which is associated with the level of MGMT expression. Evidently, schedule-dependent manipulation of signaling pathways involved in MGMT regulation and their assessment as surrogate markers are critical for overcoming resistance and predicting response to TMZ-based combination treatments in GBM.

**Conflict of interest statement** The authors declare that there are no conflicts of interest.

## References

1. Preusser M, de Ribaupierre S, Wöhrer A et al (2011) Current concepts and management of glioblastoma. *Ann Neurol* 70:9–21
2. Christmann M, Verbeek B, Roos WP, Kaina B (1816) O(6)-Methylguanine-DNA methyltransferase (MGMT) in normal tissues and tumors: Enzyme activity, promoter methylation and immunohistochemistry. *Biochim Biophys Acta* 2011:179–190
3. Xu-Welliver M, Pegg AE (2002) Degradation of the alkylated form of the DNA repair protein, O(6)-alkylguanine-DNA alkyltransferase. *Carcinogenesis* 23:823–830
4. Hegi ME, Liu L, Herman JG et al (2008) Correlation of O6-methylguanine methyltransferase (MGMT) promoter methylation with clinical outcomes in glioblastoma and clinical strategies to modulate MGMT activity. *J Clin Oncol* 26:4189–4199
5. Harris LC, Remack JS, Houghton PJ, Brent TP (1996) Wild-type p53 suppresses transcription of the human O6-methylguanine-DNA methyltransferase gene. *Cancer Res* 56:2029–2032
6. Chen FY, Harris LC, Remack JS, Brent TP (1997) Cytoplasmic sequestration of an O6-methylguanine-DNA methyltransferase enhancer binding protein in DNA repair-deficient human cells. *Proc Natl Acad Sci U S A* 94:4348–4353
7. Boldogh I, Ramana CV, Chen Z, Biswas T, Hazra TK, Grösch S, Grombacher T, Mitra S, Kaina B (1998) Regulation of expression of the DNA repair gene O6-methylguanine-DNA methyltransferase via protein kinase C-mediated signaling. *Cancer Res* 58:3950–3956
8. Biswas T, Ramana CV, Srinivasan G, Boldogh I, Hazra TK, Chen Z, Tano K, Thompson EB, Mitra S (1999) Activation of human O6-methylguanine-DNA methyltransferase gene by glucocorticoid hormone. *Oncogene* 18:525–532
9. Bhakat KK, Mitra S (2000) Regulation of the human O(6)-methylguanine-DNA methyltransferase gene by transcriptional coactivators cAMP response element-binding protein-binding protein and p300. *J Biol Chem* 275:34197–34204
10. Lavon I, Fuchs D, Zrihan D, Efroni G, Zelikovitch B, Fellig Y, Siegal T (2007) Novel mechanism whereby nuclear factor kappaB mediates DNA damage repair through regulation of O(6)-methylguanine-DNA-methyltransferase. *Cancer Res* 67:8952–8959
11. Bocangel D, Sengupta S, Mitra S, Bhakat KK (2009) p53-mediated down-regulation of the human DNA repair gene O6-methylguanine-DNA methyltransferase (MGMT) via interaction with Sp1 transcription factor. *Anticancer Res* 29:3741–3750
12. Sato A, Sunayama J, Matsuda K, Seino S, Suzuki K, Watanabe E, Tachibana K, Tomiyama A, Kayama T, Kitanaka C (2011) MEK-ERK signaling dictates DNA-repair gene MGMT expression and temozolomide resistance of stem-like glioblastoma cells via the MDM2-p53 axis. *Stem Cells* 29:1942–1951
13. Persano L, Pistollato F, Rampazzo E, Della Puppa A, Abbadi S, Frasson C, Volpin F, Indraccolo S, Scienza R, Basso G (2012) BMP2 sensitizes glioblastoma stem-like cells to TMZ by affecting HIF-1 $\alpha$  stability and MGMT expression. *Cell Death Dis* 3:e412. doi:10.1038/cddis.2012.153
14. Kohsaka S, Wang L, Yachi K, Mahabir R, Narita T, Itoh T, Tanino M, Kimura T, Nishihara H, Tanaka S (2012) STAT3 inhibition overcomes TMZ resistance in GBM by downregulating MGMT expression. *Mol Cancer Ther* 11:1289–1299
15. Zhang W, Zhang J, Hoadley K, Kushwaha D, Ramakrishnan V, Li S, Kang C, You Y, Jiang C, Song SW, Jiang T, Chen CC (2012) miR-181d: a predictive glioblastoma biomarker that downregulates MGMT expression. *Neuro Oncol* 14:712–719
16. Adams J (2003) The proteasome: structure, function, and role in the cell. *Cancer Treat Rev* 29(Suppl 1):3–9
17. Yin D, Zhou H, Kumagai T, Liu G, Ong JM, Black KL, Koeffler HP (2005) Proteasome inhibitor PS-341 causes cell growth arrest and apoptosis in human glioblastoma multiforme (GBM). *Oncogene* 24:344–354
18. Tianhu Z, Shiguang Z, Xinghan L (2010) Bmf is upregulated by PS-341-mediated cell death of glioma cells through JNK phosphorylation. *Mol Biol Rep* 37:1211–1219
19. Unterkircher T, Cristofanon S, Vellanki SH, Nonnenmacher L, Karpel-Massler G, Wirtz CR, Debatin KM, Fulda S (2011) BZ primes glioblastoma, including glioblastoma stem cells, for TRAIL by increasing tBid stability and mitochondrial apoptosis. *Clin Cancer Res* 17:4019–4030
20. Seol DW (2011) p53-Independent up-regulation of a TRAIL receptor DR5 by proteasome inhibitors: a mechanism for proteasome inhibitor-enhanced TRAIL-induced apoptosis. *Biochem Biophys Res Commun* 416:222–225
21. Kubicek GJ, Werner-Wasik M, Machtay M, Mallon G, Myers T, Ramirez M, Andrews D, Curran WJ Jr, Dicker AP (2009) Phase I

- trial using proteasome inhibitor BZ and concurrent TMZ and radiotherapy for central nervous system malignancies. *Int J Radiat Oncol Biol Phys* 74:433–439
22. Portnow J, Frankel P, Koehler S, Twardowski P, Shibata S, Martel C, Morgan R, Cristea M, Chow W, Lim D, Chung V, Reckamp K, Leong L, Synold TW (2012) A phase I study of bortezomib and temozolomide in patients with advanced solid tumors. *Cancer Chemother Pharmacol* 69:505–514
  23. Fischel JL, Formento P, Milano G (2005) Epidermal growth factor receptor double targeting by a tyrosine kinase inhibitor (Iressa) and a monoclonal antibody (Cetuximab) Impact on cell growth and molecular factors. *Br J Cancer* 92:1063–1068
  24. Voutsadakis IA, Patrikidou A, Tsapakidis K, Karagiannaki A, Hatzidaki E, Stathakis NE, Papandreou CN (2010) Additive inhibition of colorectal cancer cell lines by aspirin and bortezomib. *Int J Colorectal Dis* 25:795–804
  25. Patrikidou A, Vlachostergios PJ, Voutsadakis IA, Hatzidaki E, Valeri RM, Destouni C, Apostolou E, Daliani D, Papandreou CN (2011) Inverse baseline expression pattern of the NEP/neuropeptides and NF $\kappa$ B/proteasome pathways in androgen-dependent and androgen-independent prostate cancer cells. *Cancer Cell Int* 11:13
  26. Hirose Y, Berger MS, Pieper RO (2001) Abrogation of the Chk1-mediated G(2) checkpoint pathway potentiates temozolomide-induced toxicity in a p53-independent manner in human glioblastoma cells. *Cancer Res* 61:5843–5849
  27. Hirose Y, Berger MS, Pieper RO (2001) p53 effects both the duration of G2/M arrest and the fate of temozolomide-treated human glioblastoma cells. *Cancer Res* 61:1957–1963
  28. Bredel M, Bredel C, Juric D, Duran GE, Yu RX, Harsh GR, Vogel H, Recht LD, Scheck AC, Sikic BI (2006) Tumor necrosis factor- $\alpha$ -induced protein 3 as a putative regulator of nuclear factor- $\kappa$ B-mediated resistance to O6-alkylating agents in human glioblastomas. *J Clin Oncol* 24:274–287
  29. Roccaro AM, Vacca A, Ribatti D (2006) Bortezomib in the treatment of cancer. *Recent Pat Anticancer Drug Discov* 1:397–403
  30. Yamini B, Yu X, Dolan ME, Wu MH, Darga TE, Kufe DW, Weichselbaum RR (2007) Inhibition of nuclear factor- $\kappa$ B activity by temozolomide involves O6-methylguanine induced inhibition of p65 DNA binding. *Cancer Res* 67:6889–6898
  31. Belanich M, Randall T, Pastor MA, Kibitel JT, Alas LG, Dolan ME, Schold SC Jr, Gander M, Lejeune FJ, Li BF, White AB, Wasserman P, Citron ML, Yarosh DB (1996) Intracellular Localization and intercellular heterogeneity of the human DNA repair protein O(6)-methylguanine-DNA methyltransferase. *Cancer Chemother Pharmacol* 37:547–555
  32. Pore N, Jiang Z, Shu HK, Bernhard E, Kao GD, Maity A (2006) Akt1 activation can augment hypoxia-inducible factor-1 $\alpha$  expression by increasing protein translation through a mammalian target of rapamycin-independent pathway. *Mol Cancer Res* 4:471–479
  33. Mylonis I, Chachami G, Samiotaki M, Panayotou G, Paraskeva E, Kalousi A, Georgatou E, Bonanou S, Simos G (2006) Identification of MAPK phosphorylation sites and their role in the localization and activity of hypoxia-inducible factor-1 $\alpha$ . *J Biol Chem* 281:33095–33106
  34. Befani CD, Vlachostergios PJ, Hatzidaki E, Patrikidou A, Bonanou S, Simos G, Papandreou CN, Liakos P (2012) Bortezomib represses HIF-1 $\alpha$  protein expression and nuclear accumulation by inhibiting both PI3K/Akt/TOR and MAPK pathways in prostate cancer cells. *J Mol Med (Berl)* 90:45–54
  35. Weller M, Stupp R, Hegi ME, van den Bent M, Tonn JC, Sanson M, Wick W, Reifenberger G (2012) Personalized care in neurooncology coming of age: why we need MGMT and 1p/19q testing for malignant glioma patients in clinical practice. *Neuro Oncol* 14(Suppl 4):iv100–iv108
  36. Korkolopoulou P, Levidou G, Saetta AA, El-Habr E, Eftchiadis C, Demenagas P, Thymara I, Xiromeritis K, Boviatsis E, Thomas-Tsagli E, Panayotidis I, Patsouris E (2008) Expression of nuclear factor- $\kappa$ B in human astrocytomas: relation to pI kappa B $\alpha$ , vascular endothelial growth factor, Cox-2, microvascular characteristics, and survival. *Hum Pathol* 39:1143–1152
  37. Saetta AA, Levidou G, El-Habr EA, Panayotidis I, Samaras V, Thymara I, Sakellariou S, Boviatsis E, Patsouris E, Korkolopoulou P (2011) Expression of pERK and pAKT in human astrocytomas: correlation with IDH1-R132H presence, vascular endothelial growth factor, microvascular characteristics and clinical outcome. *Virchows Arch* 458:749–759
  38. Wang Y, Chen L, Bao Z, Li S, You G, Yan W, Shi Z, Liu Y, Yang P, Zhang W, Han L, Kang C, Jiang T (2011) Inhibition of STAT3 reverses alkylator resistance through modulation of the AKT and  $\beta$ -catenin signaling pathways. *Oncol Rep* 26:1173–1180
  39. Piperi C, Samaras V, Levidou G, Kavantzias N, Boviatsis E, Petraki K, Grivas A, Barbatis C, Varsos V, Patsouris E, Korkolopoulou P (2011) Prognostic significance of IL-8-STAT-3 pathway in astrocytomas: correlation with IL-6, VEGF and microvessel morphometry. *Cytokine* 55:387–395
  40. Mashiko R, Takano S, Ishikawa E, Yamamoto T, Nakai K, Matsumura A (2011) Hypoxia-inducible factor 1 $\alpha$  expression is a prognostic biomarker in patients with astrocytic tumors associated with necrosis on MR image. *J Neurooncol* 102:43–50
  41. Korkolopoulou P, Patsouris E, Konstantinidou AE, Pavlopoulos PM, Kavantzias N, Boviatsis E, Thymara I, Perdiki M, Thomas-Tsagli E, Angelidakis D, Rologis D, Sakkas D (2004) Hypoxia-inducible factor 1 $\alpha$ /vascular endothelial growth factor axis in astrocytomas. Associations with microvessel morphometry, proliferation and prognosis. *Neuropathol Appl Neurobiol* 30:267–278
  42. Hideshima T, Chauhan D, Hayashi T, Akiyama M, Mitsiades N, Mitsiades C, Podar K, Munshi NC, Richardson PG, Anderson KC (2003) Proteasome inhibitor PS-341 abrogates IL-6 triggered signaling cascades via caspase-dependent downregulation of gp130 in multiple myeloma. *Oncogene* 22:8386–8893
  43. Chun YS, Kim MS, Park JW (2002) Oxygen-dependent and -independent regulation of HIF-1 $\alpha$ . *J Korean Med Sci* 17:581–588
  44. Dey A, Wong E, Kua N, Teo HL, Tergaonkar V, Lane D (2008) Hexamethylene bisacetamide (HMB) simultaneously targets AKT and MAPK pathway and represses NF  $\kappa$ B activity: implications for cancer therapy. *Cell Cycle* 7:3759–3767
  45. Chen KF, Liu CY, Lin YC, Yu HC, Liu TH, Hou DR, Chen PJ, Cheng AL (2010) CIP2A mediates effects of bortezomib on phospho-Akt and apoptosis in hepatocellular carcinoma cells. *Oncogene* 29:6257–6266
  46. Ng K, Nitta M, Hu L, Kesari S, Kung A, D'Andrea A, Chen CC (2009) A small interference RNA screen revealed proteasome inhibition as strategy for glioblastoma therapy. *Clin Neurosurg* 56:107–118
  47. Fisher T, Galanti G, Lavie G, Jacob-Hirsch J, Kventzel I, Zeligson S, Winkler R, Simon AJ, Amariglio N, Rechavi G, Toren A (2007) Mechanisms operative in the antitumor activity of temozolomide in glioblastoma multiforme. *Cancer J* 13(5):335–344
  48. Brell M, Ibáñez J, Tortosa A (2011) O6-Methylguanine-DNA methyltransferase protein expression by immunohistochemistry in brain and non-brain systemic tumours: systematic review and meta-analysis of correlation with methylation-specific polymerase chain reaction. *BMC Cancer* 11:35
  49. Sonoda Y, Yokosawa M, Saito R, Kanamori M, Yamashita Y, Kumabe T, Watanabe M, Tominaga T (2010) O(6)-Methylguanine DNA methyltransferase determined by promoter hypermethylation and immunohistochemical expression is correlated with progression-free survival in patients with glioblastoma. *Int J Clin Oncol* 15:352–358
  50. Capper D, Mittelbronn M, Meyerermann R, Schittenhelm J (2008) Pitfalls in the assessment of MGMT expression and in its correlation with survival in diffuse astrocytomas: proposal of a feasible immunohistochemical approach. *Acta Neuropathol* 115:249–259

51. Christmann M, Nagel G, Horn S, Krahn U, Wiewrodt D, Sommer C, Kaina B (2010) MGMT activity, promoter methylation and immunohistochemistry of pretreatment and recurrent malignant gliomas: a comparative study on astrocytoma and glioblastoma. *Int J Cancer* 127:2106–2118
52. van Nifterik KA, van den Berg J, van der Meide WF, Ameziane N, Wedekind LE, Steenbergen RD, Leenstra S, Lafleur MV, Slotman BJ, Stalpers LJ, Sminia P (2010) Absence of the MGMT protein as well as methylation of the MGMT promoter predict the sensitivity for temozolomide. *Br J Cancer* 103:29–35
53. Szeliga M, Zgrzywa A, Obara-Michlewska M, Albrecht J (2012) Transfection of a human glioblastoma cell line with liver-type glutaminase (LGA) down-regulates the expression of DNA-repair gene MGMT and sensitizes the cells to alkylating agents. *J Neurochem* 123:428–436
54. Felsberg J, Thon N, Eigenbrod S, Hentschel B, Sabel MC, Westphal M, Schackert G, Kreth FW, Pietsch T, Löffler M, Weller M, Reifenberger G, Tonn JC, Network GG (2011) Promoter methylation and expression of MGMT and the DNA mismatch repair genes MLH1, MSH2, MSH6 and PMS2 in paired primary and recurrent glioblastomas. *Int J Cancer* 129:659–670
55. Brandes AA, Franceschi E, Tosoni A, Bartolini S, Bacci A, Agati R, Ghimenton C, Turazzi S, Talacchi A, Skrap M, Marucci G, Volpin L, Morandi L, Pizzolitto S, Gardiman M, Andreoli A, Calbucci F, Ermani M (2010) O(6)-methylguanine DNA-methyltransferase methylation status can change between first surgery for newly diagnosed glioblastoma and second surgery for recurrence: clinical implications. *Neuro Oncol* 12:283–288
56. Kreth S, Thon N, Eigenbrod S, Lutz J, Ledderose C, Egensperger R, Tonn JC, Kretschmar HA, Hinske LC, Kreth FW (2011) O-methylguanine-DNA methyltransferase (MGMT) mRNA expression predicts outcome in malignant glioma independent of MGMT promoter methylation. *PLoS One* 6:e17156